A new method for calculating the Busemann head coefficients for radial impellers

W. E. Mason*

Charts of the Busemann head coefficients which are widely used in the design of centrifugal pumps and compressors contain substantial errors. This paper presents a simplified method for evaluating these coefficients which is capable of giving results of high accuracy for impellers with two or more blades having blade angles from 10°–90°, covering most designs of practical interest. It is also shown that significant error may result from the conventional assumption that head coefficients are independent of radius ratio for values of the solidity greater than 1.0; a simple method of checking the magnitude of this error is given

Key words: *centrifugal pumps, compressors, Busemann head coefficients*

The solution obtained over 50 years ago by Busemann[1] for the head generated by potential flow through a radial impeller with blades of logarithmic spiral form has found wide application in the design and performance analysis of centrifugal pumps and compressors[2–7,9,10]. Busemann presented his solution in terms of two dimensionless head coefficients, h_0 and c_m, which are functions of the blade angle (β), the radius ratio (r_1/r_2) and the number of blades in the impeller (z).

The evaluation of these head coefficients requires the summation of two infinite series which converge slowly for those values of radius ratio and blade number which are most commonly encountered in practice. Busemann's original charts giving h_0 and c_m as functions of radius ratio with blade number as a parameter for six values of blade angle (5, 10, 20, 40, 60 and 90°) have been reproduced by several authors[2,3,8,10]; in other cases, data taken from the charts have been presented in summarized and simplified form[9,11,13].

The present work was undertaken when discrepancies were found between h_0 values read from Busemann's charts and those calculated using the analysis given in his paper. Further examination showed significant errors in the curves for low blade numbers and low blade angles on the charts; it is these curves which are of particular relevance to pump design problems.

Fig 1, which shows the form of a typical curve of h_0 versus radius ratio, indicates the position of these errors, which were found to occur at two distinct locations on the curve.

- at the steepest part of the curve (point B), where the error in h_0 approached 10% in some cases;
- at the knee of the curve (point C), where the radius of curvature shown on the charts tends to be too small, so that h_0 appears to reach its maximum at a radius ratio that is higher than the true value.

The second type of error evidently arose from the computational difficulty mentioned above; the series from which h_0 is calculated converge so slowly in this region of the chart that it would be impossible to evaluate them accurately without the use of modern computing facilities.

Corresponding errors were found to occur in Busemann's charts of the coefficient c_m; these charts, however, are not essential, as c_m can readily be calculated directly from h_0 once the value of the latter has been obtained.

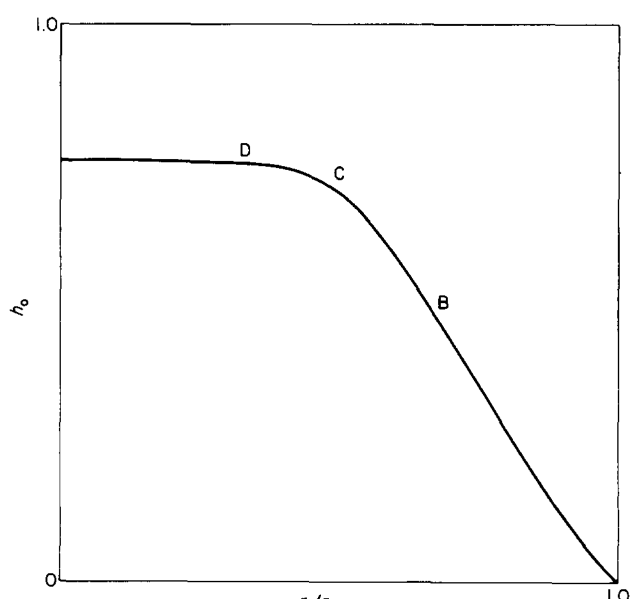

Fig 1 Typical curve of h₀ *versus radius ratio*

* Department of Chemical Engineering, National University of Singapore, Kent Ridge, Singapore 0511. Present address: School of Mechanical and Offshore Engineering, Robert Gordon's Institute of Technology, Schoolhill, Aberdeen, Scotland, AB9 1FR
Received on 22 November 1982 and accepted for publication on 17 January 1983

The errors in Busemann's charts, and other published charts derived from them, and the difficulties of interpolation for intermediate values of blade angle and blade number when charts of this type are used stimulated development of a new method to permit rapid and accurate calculation of h_0 values for the whole range of blade angles and blade numbers of practical interest using the minimum number of charts. Before describing this method in detail, Busemann's analysis will be summarized briefly.

Busemann's analysis

Busemann considered potential flow through a radial impeller with z equally-spaced blades of constant width and logarithmic spiral form with blade angle β. The flow was built up by superposition of three flow patterns:

- a through-flow consisting of a spiral vortex representing the absolute flow through the stationary impeller;
- a displacement flow which is the fluid motion resulting from rotation of the impeller at zero throughflow;
- a circulation round each blade which is adjusted to ensure that the flow pattern resulting from the superposition satisfies the Kutta condition.

The potential representing the superposed flow pattern is obtained by a conformal transformation which maps the front and rear surfaces of each impeller blade, drawn in the ζ plane, onto the entire circumference of a unit circle in the w plane (Fig 2).

The origin in the ζ plane, located on the impeller axis, is represented by the point w_0 in the w plane, while points w_1 and w_2 represent the leading and trailing edges of the blades respectively. The value

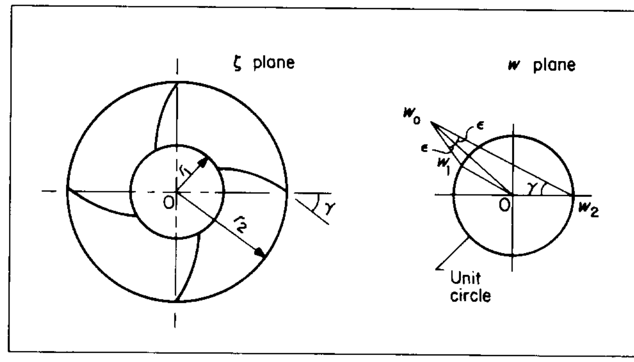

Fig 2 Geometry of Busemann's conformal transformation

of r_2, the radius at the blade outlet, is taken as unity without loss of generality. The conformal transformation employed is;

$$z \ln \zeta = \ln\left(\frac{w_0 - w}{w_0 - 1}\right) + e^{2i\gamma} \ln\left(\frac{\bar{w}_0 - 1/w}{\bar{w}_0 - 1}\right) \qquad (1)$$

where $\gamma = \pi/2 - \beta$ and angles are expressed in radians. The dimensionless impeller head h is defined by the relation:

$$h = \frac{gH}{u_2^2}$$

where H is the head generated, g the gravitational acceleration and u_2 the tangential velocity of the blades at the outlet radius. The dimensionless head is given by:

$$h = h_0 - h_\nu \varphi(\cot\beta - \cot\beta_1) \qquad (2)$$

where β is the blade angle, β_1 the angle (measured with respect to the tangential direction) of the

Notation

For convenience, the notation of Busemann's original paper[1] is followed for the most part.

a	$1/w_0$
c_m	Head coefficient (Eq 11)
g	Gravitational acceleration
h	Dimensionless impeller head, gH/u_2^2
H	Impeller head
h_0, h_ν	Head coefficients given by Eqs 3 and 5 respectively
k	Constant in Eq 15
m	$4\cos^2\gamma/z^2$
M	$S_1 + zS_2(1-h_\nu)/h_\nu$(Eq 17)
N	Function of ε and γ given by Eq 6
q	Function of γ and z given by Eq 9
S_1, S_2	Series given by Eq 7 and Eq 8 respectively
$\bar{S}_1$	Euler's constant (0.577216)
$\bar{S}_2, \bar{S}_3$ etc.	Sums of series of reciprocal powers
u	Circumferential velocity of a point on an impeller blade
v_r	Radial component of fluid velocity
w	Complex co-ordinates in the w plane (Fig 2)
z	Number of blades in the impeller
α	Constant in Eq 15
β	Blade angle measured with respect to the backward-pointing tangent
γ	$\pi/2 - \beta$
ε	Angle in Fig 2
ζ	Complex co-ordinates in the ζ plane (Fig 2)
θ	Function of ε and γ given by Eqs 20 or 21
σ	Solidity, $z \ln(r_2/r_1)/2\pi\cos\gamma$
φ	Flow coefficient, v_{r2}/u_2

Subscripts

0	Refers to impeller axis
1	Refers to blade inlet
2	Refers to blade outlet

The prime superscript (′) indicates that the quantity concerned is evaluated for the special case of $\varepsilon = \gamma$

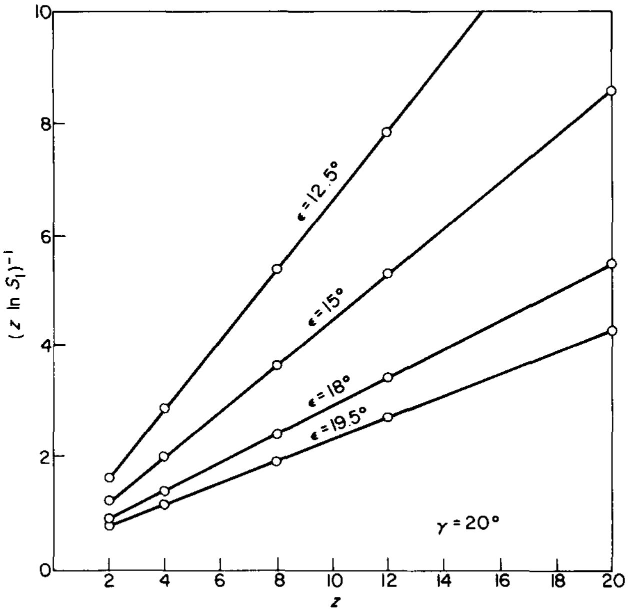

Fig 3 $(z \ln S_1)^{-1}$ *versus* z *for* $\gamma = 20°$

absolute flow entering the impeller, and φ is the flow coefficient (given by v_{r2}/u_2 where v_{r2} is the radial component of the velocity of the fluid leaving the impeller). The head coefficient h_0 is then given in terms of the series S_1 and S_2 by:

$$h_0 = \frac{h_\nu S_1 + z(1-h_\nu)S_2}{N} \tag{3}$$

h_ν and N are most conveniently expressed in terms of the parameter ε. It can be seen from Fig 2 that if $a = 1/w_0$ then $|a| = \sin\varepsilon/\sin\gamma$. ε is related to z and the radius ratio by:

$$z \ln(r_2/r_1) = 2\cos^2\gamma \times\left[2\varepsilon \tan\gamma - \ln\left(\frac{\sin(\gamma-\varepsilon)}{\sin(\gamma+\varepsilon)}\right)\right] \tag{4}$$

Then h_ν and N are given by:

$$h_\nu = \frac{2\sin\varepsilon\cos\gamma}{\sin(\gamma+\varepsilon)} \tag{5}$$

$$N = \exp\left\{\frac{4\cos^2\gamma}{z}\left[\varepsilon\tan\gamma + \ln\left(\frac{\sin(\gamma+\varepsilon)}{\sin\gamma}\right)\right]\right\} \tag{6}$$

The series S_1 and S_2 are:

$$S_1 = \sum_{l=0}^{\infty}\binom{q}{l}\binom{\bar{q}}{l}|a|^{2l} = 1 + m\left[|a|^2 + \frac{(1-mz+m)}{2^2}|a|^4 + \frac{(1-mz+m)(4-2mz+m)}{2^2(3^2)}|a|^6 + \cdots\right] \tag{7}$$

$$S_2 = \sum_{l=0}^{\infty} l\binom{q}{l}\binom{\bar{q}}{l}|a|^{2l} = m\left[|a|^2 + \frac{(1-mz+m)}{2}|a|^4 + \frac{(1-mz+m)(4-2mz+m)}{2^2(3)}|a|^6 + \cdots\right] \tag{8}$$

where

$$q = \frac{1+e^{-2i\gamma}}{z} \tag{9}$$

and

$$m = \frac{4\cos^2\gamma}{z^2} \tag{10}$$

For evaluating Eq (2), Busemann provides charts of the coefficients h_0 and c_m plotted versus radius ratio, with z as a parameter, where c_m is given by:

$$c_m = h_0/h_\nu \tag{11}$$

It seems preferable, however, to make use of h_ν directly since this is independent of z, unlike c_m. Note that as the number of blades becomes very large, $S_1 \to 1.0$, $zS_2 \to 0$ and $N \to 1.0$, so $h_0 \to h_\nu$.

Evaluation of h_0

The method used to evaluate h_0 here is to approximate the series S_1 and S_2 by power series in z^{-1} which converge rapidly for those values of z which are of practical interest, ie for $z \geq 2$.

The principle may be illustrated by considering the evaluation of S_1 for the case of $\varepsilon = \gamma$; this value will be denoted by S'_1. (The addition of a prime to a symbol indicates that the quantity concerned is evaluated for the case of $\varepsilon = \gamma$.)

For $\varepsilon = \gamma$, $|a| = 1.0$; both S_1 and S_2 then reduce to examples of the hypergeometric series and may be expressed in terms of gamma functions:

$$S'_1 = zS'_2 = \frac{\Gamma(1+q+\bar{q})}{\Gamma(1+q)\Gamma(1+\bar{q})} \tag{12}$$

Note that since for $\varepsilon = \gamma$, $h_\nu = 1.0$, the value of S'_2 is not required to evaluate h'_0. This expression may be evaluated from published tables, such as those of Abramov[14], but for these purposes it is more convenient (see, for example, Luke[15]) to make use of the relation:

$$\ln\Gamma(z+1) = \sum_{k=1}^{\infty}(-1)^k\bar{S}_k z^k/k \qquad (|z|<1) \tag{13}$$

to express $\ln(S'_1)$ as a power series in z^{-1}:

$$\ln(S'_1) = \frac{4\cos^2\gamma}{z^2}\left[\bar{S}_2 - \frac{4\cos^2\gamma}{z}\bar{S}_3 + \frac{4\cos^2\gamma}{z^2}(8\cos^2\gamma - 1)\bar{S}_4 + \cdots\right] \tag{14}$$

where $\bar{S}_1$ is Euler's constant, and $\bar{S}_2$, $\bar{S}_3$ etc are the sums of series of reciprocal powers. For $z \geq 2$, this series converges rapidly and can be represented accurately by the simple expression

$$\ln(S'_1) = \frac{\alpha'}{z(z+\alpha'k')} \tag{15}$$

where the constants α' and k$'$ are functions of γ. Taking α' as $4\cos^2\gamma(\bar{S}_2)$ $(=6.580\cos^2\gamma)$, the values of k$'$ giving the best fit were obtained by linear regression from plots of $[z\ln(S'_1)]^{-1}$ versus z (Fig 3), using values of S'_1 computed from Eq (12). The dependence of k′ on cos γ was found to be given by:

$$k = 0.553 - 0.134 \cos\gamma \tag{16}$$

Since $\ln(S_1)$ is approximately proportional to $|a|^2$ for fixed values of γ and z, the above procedure may be extended to values of ε less than γ. Now for $z \to \infty$ we have:

$$S_1 \to 1.0$$

$$S_2 \to \frac{-4\cos^2\gamma}{z^2} \ln(1-|a|^2) \qquad (\ll 1)$$

so for large values of z^2 the numerator of Eq (3) may be written:

$$\ln M = \ln S_1 - \frac{4\cos^2\gamma}{z}\left(\frac{1-h_\nu}{h_\nu}\right) \ln(1-|a|^2) \tag{17}$$

where

$$M = S_1 + zS_2(1-h_\nu)/h_\nu$$

By incorporating an expression of the form of Eq (15) in Eq (17) the following relation is obtained which is found to represent $\ln M$ with high accuracy for $z \geqslant 2$:

$$z \ln M = \frac{\alpha}{z + \alpha k} - 4\cos^2\gamma[(1-h_\nu)/h_\nu] \ln(1-|a|^2) \tag{18}$$

Fig 4, in which the plotted points were obtained by direct computation of S_1 and S_2, illustrates the effectiveness of this method of representation.

Eq (18) may then be put in the form:

$$z \ln(h_0/h_\nu) = \frac{\alpha}{z+\alpha k} - \theta \tag{19}$$

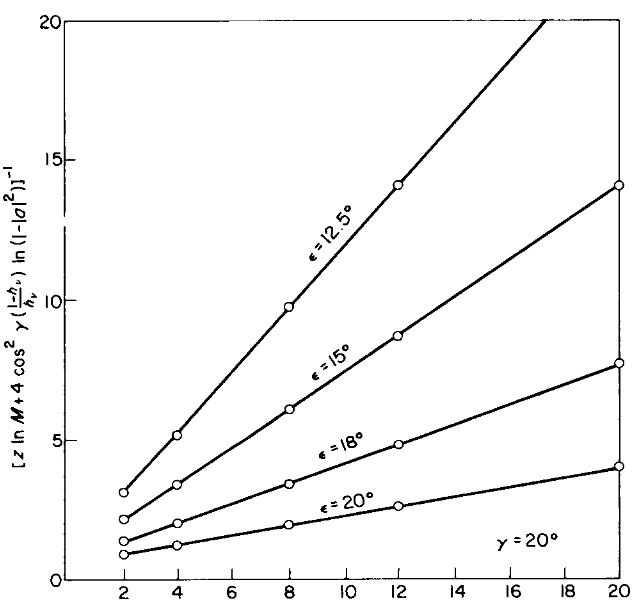

Fig 4 $\left[z \ln M + 4\cos^2\gamma\left(\frac{1-h_\nu}{h_\nu}\right)\ln(1-|a|^2)\right]^{-1}$ *versus* z *for* $\gamma = 20°$

where θ is a function of ε and γ most readily obtained from:

$$\theta = z\ln(r_2/r_1) + \frac{2\cos\varepsilon\cos\gamma}{|a|}\ln(1-|a|^2) \qquad (\text{for } |a|<1) \tag{20}$$

$$\theta = \theta' = 4\cos^2\gamma[\ln(2\cos\gamma) + \gamma\tan\gamma] \qquad (\text{for } |a|=1) \tag{21}$$

Eq (19) provides a convenient approach for the calculation of h_0, since the quantities h_ν, θ, and k are functions of ε and γ only. The procedure is therefore much simpler than that for the exact calculation, which requires the series S_1 and S_2 to be evaluated for each value of z.

The values of α and k for use in Eq (19) are obtained from charts of α/α' versus $|a|^2$ and k/k′ versus h_ν (reproduced in Figs 5 and 6 respectively) prepared by linear regression of plots such as that shown in Fig 4, the values of M being obtained by direct computation of S_1 and S_2. The value of α must be determined with greater precision than is possible using a small-scale reproduction such as that given in Fig 5, and for this purpose the curve for α may be represented by Eqs (22) or (23) for the ranges of $|a|^2$ indicated; values of the coefficients c_1, c_2 etc in Eq (23) are shown in Table 1.

$$\alpha/\alpha' = 1 - 2.06(1-|a|^2)^{0.69} \qquad (1.0 \geqslant |a|^2 \geqslant 0.95) \tag{22}$$

$$\alpha/\alpha' = c_1|a|^2 + c_2|a|^4 + c_3|a|^6 + c_4|a|^8 \qquad (0.95 \geqslant |a|^2 \geqslant 0) \tag{23}$$

In Fig 6, separate curves are required for the ranges of γ shown for values of h_ν greater than 0.78; for $30° > \gamma > 20°$ interpolation is required. Eq (24) holds for all values of γ when h_ν is less than 0.78:

$$k/k' = 2.664 - 1.760h_\nu \quad (h_\nu < 0.78) \tag{24}$$

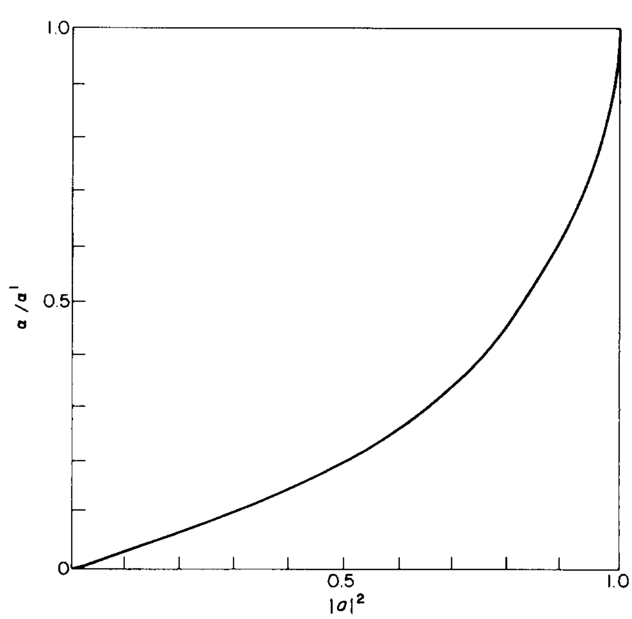

Fig 5 α/α' *as a function of* a

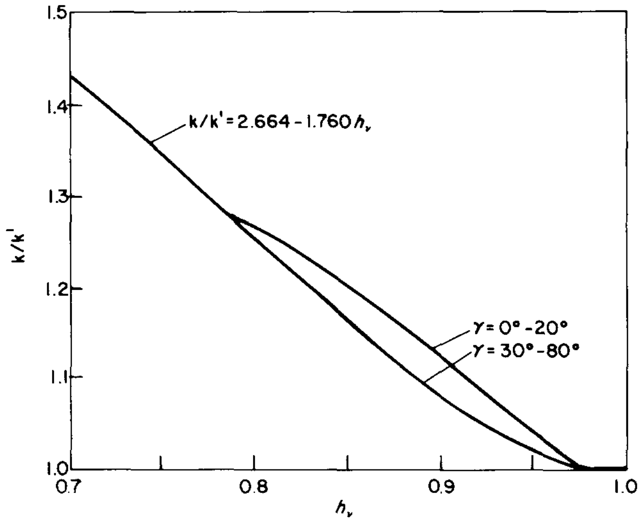

Fig 6 k/k' *versus* h_ν

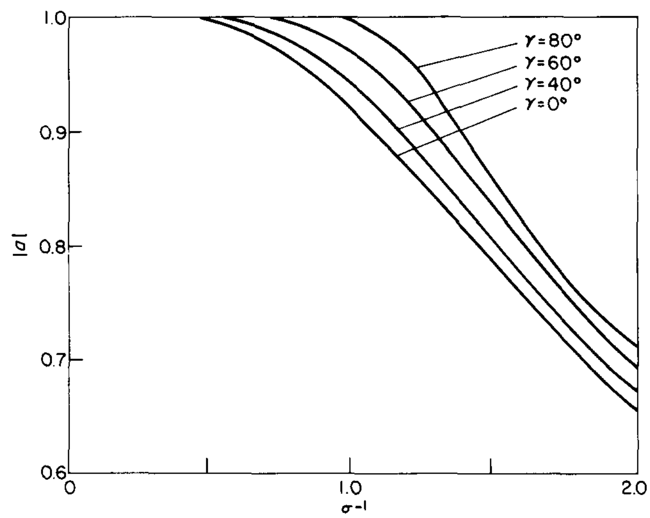

Fig 7 |a| *versus* σ^{-1} *with* γ *as a parameter*

To summarize, the procedure for calculating the Busemann coefficients h_0 and h_ν for an impeller of given geometry is:

1. Calculate the value of $z \ln (r_2/r_1)$ for the impeller.
2. Obtain the corresponding value of ε. Except for the case of radial blades ($\gamma = 0°$) this requires a trial-and-error calculation, since Eq (4) cannot be made explicit in ε. A first estimate of ε may be obtained from Fig 7 which gives $|a|$ as a function of the reciprocal of the solidity, σ, with γ as a parameter. (Solidity, σ, is defined by $\sigma = z \ln (r_2/r_1)/2\pi \cos \gamma$.) For values of $|a|$ less than 0.7, the following approximation is useful:

$$\varepsilon = \tan \gamma \tan h\left(\frac{z \ln (r_2/r_1)}{4}\right) \text{ (radians)} \tag{25}$$

3. Calculate α' ($\alpha' = 6.580 \cos^2 \gamma$) and obtain k' from Eq (16).
4. Obtain the value of α/α' from Eq (22) or (23) as appropriate and k/k' from Fig 6.
5. Calculate θ from Eq (20), and then obtain h_0 from Eq (19).

For the case of $\varepsilon = \gamma$, $h_\nu = 1.0$ and $h_0 = h_0'$, α' and k' are calculated as in step (3) above, and θ is obtained from Eq (21); h_0 is then given by:

$$z \ln h_0' = \frac{\alpha'}{z + \alpha' k'} - \theta' \tag{26}$$

For radial blades the procedure is simplified, since $\varepsilon = \gamma = 0°$, so that $|a|$ and h_ν may be obtained directly from:

$$z \ln (r_2/r_1) = 2 \ln \left(\frac{1+|a|}{1-|a|}\right) \qquad (\gamma = 0°) \tag{27}$$

$$h_\nu = \frac{2|a|}{1+|a|} \qquad (\gamma = 0°) \tag{28}$$

Table 1 Values of the coefficients for Eq (23)

Range of $\lvert a\rvert^2$	c_1	c_2	c_3	c_4
$0.95 \geq \lvert a\rvert^2 \geq 0.80$	−7.4862	29.3373	−36.6756	15.7383
$0.80 \geq \lvert a\rvert^2 \geq 0.50$	−0.0733	2.0938	−3.3230	2.1372
$0.50 \geq \lvert a\rvert^2 \geq 0$	0.2848	0.2938	−0.5071	0.8406

h_0 is then obtained by carrying out steps, 4, 5 and 6 as above.

Accuracy of the method

Comparison of the approximate values of h_0 calculated by the above method with the exact values obtained by summation of the series S_1 and S_2 showed excellent agreement; the difference between the two sets of values did not exceed 0.25% for impellers with two or more blades having values of γ between 0° and 80° (ie blade angles from 90° to 10°). Table 2 shows values for some representative cases, and also includes the corresponding values read from Busemann's charts for comparison.

The points for which data are given in the table lie close to the knee of the curve of h_0 versus radius ratio. In this region, which is of particular relevance to pump design, the Busemann charts are most liable

Table 2 Values of h_0 obtained by various methods

Radius ratio, r_1/r_2	Values* of h_0		
	a	b	c
$\gamma = 0°, z = 8$			
0.400	0.758	0.758	0.77
0.479	0.750	0.750	0.77
0.534	0.740	0.739	0.75
0.577	0.726	0.726	0.74
0.615	0.710	0.710	0.71
$\gamma = 70°, z = 2$			
0.364	0.560	0.561	0.60
0.400	0.538	0.538	0.58
0.429	0.515	0.515	0.56
0.472	0.477	0.477	0.49
$\gamma = 80°, z = 4$			
0.765	0.758	0.758	0.73
0.781	0.674	0.674	0.61
0.799	0.566	0.566	0.51
0.828	0.419	0.419	0.41

* a, Exact values from sums S_1 and S_2; b, Values from Eq (19); c, Values from Busemann's charts

to error and the series S_1 and S_2 converge so slowly that several thousand terms must be taken for accurate evaluation.

Limiting solidity

The coefficient h_0 reaches its maximum value of h'_0 at a radius ratio of zero, corresponding to infinite solidity for a finite number of blades, and remains very close to this maximum for low radius ratios (Fig 1). The location of the point at which h_0/h'_0 begins to fall significantly below unity (point D in Fig 1) is a matter of some importance in pump design calculations. From an analysis of Busemann's charts, Wislicenus[2] concluded that this point is at a radius ratio corresponding to unity solidity, ie at $r_1/r_2 = \exp(-2\pi \cos \gamma/z)$, and that for all solidities greater than this limiting value the ratio h_0/h'_0 may be taken as unity with negligible error, leading to major simplifications in calculations. Wislicenus' conclusions have been adopted by most subsequent workers; in some cases it has been argued that a slightly higher value should be used for the limiting solidity, such as 1.1 or 1.3 instead of 1.0[9–14].

A re-examination of the data, taking into account the corrections made in the present work, shows that the limiting solidity varies somewhat with the values of γ and z; data for the case of $\gamma = 70°$ are shown in Table 3. A similar pattern of variation is found to exist for other values of γ.

It is clear from Table 3 that substantial errors may result if the limiting solidity is taken as 1.0 following Wislicenus, particularly at high blade numbers. The error increases with increasing z up to a maximum, the value of which may readily be found for any desired solidity by the use of Eq (19) as follows. For the case of $\varepsilon = \gamma$, we have $\theta = \theta'$ and $h_\nu = 1.0$; then it follows that:

$$\ln(h_0/h'_0) = \ln h_\nu - \frac{1}{z}\left[\theta - \theta' + \frac{\alpha'}{z+\alpha' k'} - \frac{\alpha}{z+\alpha k}\right] \tag{29}$$

from which it can be seen that for large z:

$$h_0/h'_0 = h_\nu \tag{30}$$

This gives the upper limit of the error arising from the assumption that $h_0 = h'_0$ for the value of the solidity corresponding to h_ν: eg for the case of $\gamma = 70°$ and $\sigma = 1.0$, $h_\nu = 0.9340$ and therefore the upper limit of the error is 6.6%, which is slightly greater than the value of 6.2% for $z = 20$ as shown in Table 3.

Table 4 shows the values of solidity at which $h_\nu = 0.99$ for varous values of γ; when the solidity of an impeller exceeds that given in the table for the value of γ concerned, h_0 will be within 1.0% of h'_0 for all blade numbers.

It can be seen that for solidities greater than 1.5, as is usually the case with centrifugal pump impellers, the assumption that $h_0 = h'_0$ will be reasonably accurate in all cases. For solidities less than 1.5, eg impellers with few blades and large radius ratios, Table 4 or Eq (30) will indicate whether this assumption is acceptably accurate or whether it is desirable to undertake the slightly longer calculation required to evaluate h_0 directly.

Table 3 Errors related to limiting solidity assumptions for $\gamma = 70°$

Blade number, z	% error in taking $h_0 = h'_0$ for $\sigma = 1.0$	Value of σ for which $h_0/h'_0 = 0.99$
2	2.8%	1.09
4	4.2%	1.15
8	5.1%	1.20
12	5.6%	1.21
20	6.2%	1.22

Table 4 Solidity values for $h_\nu = 0.99$

γ	σ for $h_\nu = 0.99$
0°	1.47
10°	1.46
20°	1.45
30°	1.43
40°	1.40
50°	1.36
60°	1.31
70°	1.23
80°	1.13

Csanady[11] gives a chart for the evaluation of h'_0 based on Busemann's data, and this is reproduced by Ferguson[9] and Dixon[12]. It should be noted that this chart is not accurate for high values of h'_0; the curve for $h'_0 = 0.90$, for example, gives a value of z about 11% low for a blade angle of 30°. The chart given by Sabersky and Acosta[13] also contains some inaccuracies at low blade angles. As an alternative to the use of these charts, the required values can readily be obtained by the use of Eq (19).

Conclusion

The approximation technique described in this paper provides a convenient and accurate method of calculating values of the Busemann head coefficients for radial impellers with two or more blades and blade angles from 10° to 90°, ie over the whole range of these variables likely to be encountered in practice. It gives results in close agreement with those obtained by the exact calculation while being much less cumbersome to use than the latter, which requires the slowly-converging series S_1 and S_2 to be evaluated separately for each value of blade number and blade angle. Evaluation of the head coefficients from Busemann's charts or the other published charts derived from them is unreliable for low blade numbers as a result of the errors in the original publication and the difficulties of the interpolation usually required. The method described is particularly convenient when it is necessary to examine the effect of small changes in blade angle, as in the technique for evaluation of pump model test data developed by Nixon and Otway[7].

References

1. **Busemann A.** Das Förderhöhenverhältnis radialer Kreiselpumpen mit logarithmisch-spiraligen Schaufeln. *Z. angew. Math Mech. 1928,* 8*(5) 372–384*
2. **Wislicenus G. F.** Fluid Mechanics of Turbo-Machinery, Vol. 1 *2nd edn. Dover, New York, 1965*
3. **Kovats A.** Design and Performance of Centrifugal and Axial Flow Pumps and Compressors, *Pergamon, Oxford, 1964*
4. **Osborne W. C. and Morelli D. A.** Head and Flow Observations on a High-Efficiency Free Centrigugal Pump Impeller. *Trans. Am. Soc. Mech. Engrs, 1950,* **72**, *99–107*
5. **Acosta A. J. and Bowerman R. D.** An Experimental Study of Centrifugal Pump Impellers. *Trans. Am. Soc. Mech. Engrs, 1957,* **79**, *1821–1839*
6. **Worster R. C.** The Flow in Volutes and its Effect on Centrifugal Pump Performance. *Proc. Instn Mech. Engrs, 1963,* **177***(31) 843–875*
7. **Nixon R. A. and Otway F. O. J.** The Use of Models in Determining the Performance of Large Circulating Water Pumps. *A Conference on Site Testing of Pumps, 24/26 Oct 1972 Institution of Mechanical Engineers, London*
8. **Hawthorne W. R.** (ed). Aerodynamics of Turbines and Compressors, *Princeton Univ. Press, Princeton, 1964*
9. **Ferguson T. B.** The Centrifugal Compressor Stage, *Butterworths, London, 1963*
10. **Wiesner F. J.** A Review of Slip Factors for Centrifugal Impellers. *A.S.M.E. Paper No. 66-WA/FE-18*
11. **Csanady G. T.** Head Correction Factors for Radial Impellers. *Engineering* (*London*), *1969,* **190**, *195*
12. **Dixon S. L.** Fluid Mechanics and Thermodynamics of Turbomachinery, *3rd edn, Pergamon, Oxford, 1978*
13. **Sabersky R. H., Acosta A. J. and Hauptmann A. G.** Fluid Flow, *2nd end, Macmillan, New York, 1971*
14. **Sheets H. E.** The Flow through Centrifugal Compressors and Pumps. *Trans. Am. Soc. Mech. Engrs, 1950,* **72**, *1009–1015*
15. **Abramov A. A.** Tables of $\ln \Gamma(z)$ for Complex Argument, *Pergamon, Oxford, 1960*
16. **Luke Y. L.** The Special Functions and their Approximations, *Academic Press, New York, 1969*

BOOK REVIEWS

Thermal Energy Storage

Ed. G. Beghi

(Lectures of a Course held at the Joint Research Centre, Ispra, Italy, June 1981)

I am somewhat cynical about published 'summer course' Proceedings which are expensive to buy and usually contain a 'mixed bag of goodies'. These Proceedings are no different; too many of the papers have the air of déja-vu and seem no more than non-critical, somewhat superficial overviews of the work of others, perhaps were only written as a means of obtaining travel funds to a geographically more interesting location than the author's domicile.

There is the usual, expected coverage: storage of sensible heat and of latent heat; storage by chemical and by physical means; district heating; materials for heat storage; working fluids for heat transfer; and a discussion of where the heat (thermal energy) sources are.

Of all 18 papers in this 506 page volume, I found the following papers of value and worthy of mention:

- *Abhat: Low temperature latent heat thermal energy storage.* This contains a discussion of the ideal properties of appropriate materials and a review of what is actually available, of the experimental techniques used for determining their thermal properties, and of the problems that arise, as a consequence of low thermal conductivity, in heat exhanger construction.
- *Van Velzen: Chemical heat pipes.* These use the bond energies of reversible chemical reactions (including thermal dissociation) that are endothermic for charging and exothermic for discharging. Although sensible heat losses during transportation are avoided, there are availability and separation losses that, combined with over-riding economic factors, give unacceptably low efficiencies.
- *Tabor: Short and long term storage in solar ponds.* A theoretical analysis of both short and long term storage in the suppressed, ie non-converting, pond using pond bottom storage allowing for heat transfer between pond and ground.
- *Wood: Thermal energy storage for recovery of industrial waste heat.* This contains a useful review of the industrial scene with respect to waste heat sources: working fluids, temperature levels and temporal mis-match of supply and demand. Specific consideration is given to the energy profiles of eleven industries and their potential for waste heat recovery using either high temperature regenerators, steam accumulators or hot water storage.
- *Gilli/Beckmann: Thermal energy storage for Peaking Power Generation.* An interesting overview of using steam accumulators for subsequent steam generation or feed water heating, or both, in the steam turbine cycle or compressed air energy storage for use in gas turbines. Surprising omission of key references.
- *Hadvig: Transmission of heat using hot water pipes.* Essentially a theoretical analysis of heat losses from district heating pipeworks, with both simple and complex network geometry, as a function of their insulation and the annual variation of the surface temperature of the ground. In addition economic considerations of construction